

## 16. NEOGENE CALCAREOUS NANNOFOSSILS: WESTERN MEDITERRANEAN BIOSTRATIGRAPHY AND PALEOCLIMATOLOGY<sup>1</sup>

William G. Siesser<sup>2</sup> and Eric P. de Kaenel<sup>3</sup>

### ABSTRACT

Six sites (974–979) in the western Mediterranean were investigated during Leg 161. Calcareous nannofossils are mostly abundant and well preserved in sediments recovered at all six sites, allowing detailed stratigraphic resolution. The Neogene intervals cored in Holes 974B and 975B range from upper Miocene (Messinian; Zone NN11) to upper Pliocene (Gelasian; Zone NN19A). In Hole 976B, the Neogene sequence cored ranges from middle Miocene (Serravallian; NN7) to upper Pliocene (Zone NN19A). A disconformity exists in the upper Miocene (indicated by the absence of Zones NN9 and NN10) and in the Pliocene (indicated by the absence of Zones NN13–NN17). The Neogene stratigraphic interval in Hole 977A ranges from middle or upper Miocene (Zone NN7–NN11) to upper Pliocene (NN19A). A brief hiatus occurs at the Zone NN13/NN14 boundary. The sedimentary sequence cored in Hole 978A terminated in the upper Miocene (Zone NN11). All NN11 to NN19A zones are present. Hole 979A terminated in the middle Pliocene (Zone NN16A). All Pliocene zones from NN16A to NN19A are present, although a brief Zone NN17 intrazonal hiatus is inferred based on foraminifer and nannofossil co-occurrences.

The ratio of warm-water *Discoaster brouweri* to cool-water *Coccolithus pelagicus* was used to assess changing Pliocene surface-water temperatures. All holes show a dramatic cooling beginning by Zone NN18 in the late Pliocene. Relatively cool periods also occur during the early Pliocene in early Zone NN12 and in late Zone NN13. Generally warm-water intervals occur in most holes in the early Pliocene in the late Zone NN12–early Zone NN13 and NN15 intervals and in the middle Pliocene in Zones NN16A and NN16B. The warmest period in the Pliocene was a brief interval in the middle Pliocene from late Zone NN16A to latest Zone NN16B (about 3.0 Ma to 2.6 Ma).

### INTRODUCTION

The western Mediterranean comprises the Tyrrhenian, Ligurian, Balearic, and Alboran Seas. The main objectives of Ocean Drilling Program (ODP) Leg 161 (May–July 1995) were to investigate the tectonic history and paleoceanography of the western Mediterranean. To accomplish these goals, 16 holes were drilled at six sites (Fig. 1), recovering 3565 m of sediments and sedimentary rocks, and 310 m of metamorphic rocks. One site was occupied in the Tyrrhenian Sea (Site 974), one in the Balearic Sea (Site 975), and four sites in the Alboran Sea (Sites 976, 977, 978, and 979; Fig. 1).

Integrated geological studies rely on a refined stratigraphic framework for placing tectonic and paleoceanographic events in an accurate chronostratigraphic context. Our main purpose in this paper is to provide a refined stratigraphy for the Neogene of the western Mediterranean on the basis of calcareous nannofossils; de Kaenel et al. (Chap. 13, this volume) complement this study by documenting the biostratigraphy of the Quaternary. We shall, in addition, comment on certain paleoclimatic aspects of the western Mediterranean on the basis of nannofossils in the cores. Sedimentology, lithostratigraphy, and other details of the sites described here are discussed in the Leg 161 *Initial Reports* volume (Comas, Zahn, Klaus, et al., 1996).

### METHODS

We prepared slides of core samples using a settling technique that produces a concentrated assemblage of nannofossils in a relatively

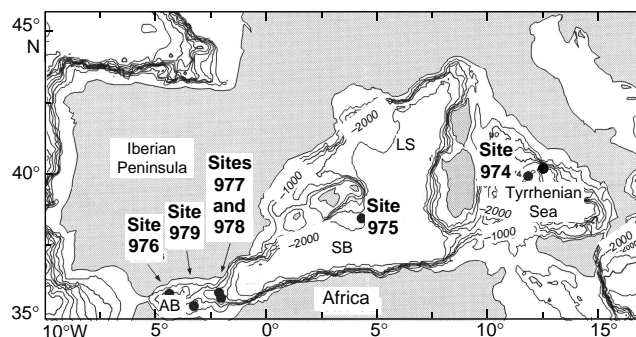


Figure 1. Location map showing Leg 161 drill sites in the Western Mediterranean. AB = Alboran Basin, SB = South Balearic Basin, LS = Ligurian Sea. Contours are in meters below sea level. Map is from Comas, Zahn, Klaus, et al. (1996).

short time. A small amount (5–10 mm<sup>3</sup>) of sediment was placed in a vial containing 13 mL of a 5% Calgon solution with a pH of 8.4. The sediment was disaggregated by gentle up-and-down crushing, then allowed to stand for 90 s, after which the upper 6 mL was drawn off and discarded. The vial was then topped up with Calgon solution and allowed to stand for 30 s. A disposable pipette was inserted into the vial to a depth of 2.0 cm and the nannofossil-bearing suspension drawn off from that depth. (A slightly different-sized vial and therefore different settling times were used aboard ship for preparation of core-catcher samples.) This crude settling technique removes much of the sediment that is coarser than 30  $\mu$ m and finer than 2  $\mu$ m from the sample, giving a “cleaner” concentration of nannofossils. The nannofossil-bearing suspension was spread evenly on a 22-x-40-mm cover glass that had previously been moistened with saliva to prevent the suspension from puddling. The suspension was dried slowly at 60°C, then the cover glass was fixed to a glass slide using Norland Optical Adhesive 61 and long-wave UV light.

<sup>1</sup>Zahn, R., Comas, M.C., and Klaus, A. (Eds.), 1999. *Proc. ODP, Sci. Results*, 161: College Station, TX (Ocean Drilling Program).

<sup>2</sup>Department of Geology, Vanderbilt University, Nashville, TN 37235, U.S.A. [siesser@ctrvax.vanderbilt.edu](mailto:siesser@ctrvax.vanderbilt.edu)

<sup>3</sup>Florida State University, Department of Geology, Tallahassee, Florida 32306, U.S.A. (Present address: Institut de Geologie Universite de Neuchâtel; Rue Emil-Argand 11, Case Postale 2; Ch 2007 Neuchâtel, Switzerland.)

**Table 1. Calcareous nannofossils considered herein, listed alphabetically by generic epithet.**

<i>Amaurolithus amplificus</i> (Bukry & Percival) Gartner & Bukry 1975	<i>Amaurolithus amplificus</i> (Bukry & Percival) Gartner & Bukry 1975
<i>Amaurolithus delicatus</i> Gartner & Bukry 1975	<i>Lithostromation perdurum</i> Deflandre 1942
<i>Amaurolithus primus</i> (Bukry & Percival) Gartner & Bukry 1975	<i>Pontosphaera indoceanica</i> Cepek 1973
<i>Amaurolithus tricorniculatus</i> (Gartner) Gartner & Bukry 1975	<i>Pontosphaera japonica</i> (Takayama) Nishida 1971
<i>Braarudosphaera bigelowii</i> (Grad & Braarud) Deflandre 1947	<i>Pontosphaera multipora</i> (Kamptner) Roth 1970
<i>Calcidiscus leptoporus</i> (Murray & Blackman) Loeblich & Tappan 1978	<i>Pseudoeumilania lacunosa</i> (Kamptner) Gartner 1969
<i>Calcidiscus macintyreii</i> (Bukry & Bramlette Loeblich & Tappan 1978	<i>Pyrocyclus hermosus</i> Roth & Hay in Hay et al. 1967
<i>Calcidiscus tropicus</i> Kamptner emend. Gartner 1992	<i>Reticulofenestra gelida</i> (Geitzenauer) Backman 1978
<i>Ceratolithus armatus</i> Muller 1974	<i>Reticulofenestra haqii</i> Backman 1978
<i>Ceratolithus cristatus</i> Kamptner 1950	<i>Reticulofenestra minuta</i> Roth 1970
<i>Ceratolithus rugosus</i> Bukry & Bramlette 1968	<i>Reticulofenestra minutula</i> (Gartner) Haq & Berggren 1978
<i>Coccolithus miopelagicus</i> Bukry 1971	<i>Reticulofenestra pseudoumbilicus</i> (Gartner) Gartner 1969
<i>Coccolithus pelagicus</i> (Wallich) Schiller 1930	<i>Reticulofenestra rotaria</i> Theodoridis 1984
<i>Coccolithus streckerii</i> Takayama & Sato 1987	<i>Rhabdosphaera claviger</i> Murray & Blackman 1898
<i>Coronocyclus nitescens</i> (Kamptner) Bramlette & Wilcoxon 1967	<i>Rhabdosphaera procera</i> Martini 1969
<i>Crenalithus doronocoides</i> (Black & Barnes) Roth 1973	<i>Scapholithus fossilis</i> Deflandre in Deflandre & Fert 1954
<i>Cryptococcolithus mediaperforatus</i> (Varol) de Kaenel 1996	<i>Scyphosphaera abelei</i> Rade 1975
<i>Cyclicargolithus floridanus</i> (Roth & Hay) Bukry 1971	<i>Scyphosphaera aequatorialis</i> Kamptner 1963
<i>Dictyococcites perplexus</i> Burns 1975	<i>Scyphosphaera amphora</i> Deflandre 1942
<i>Dictyococcites productus</i> (Kamptner) Backman 1980	<i>Scyphosphaera ampla</i> Kamptner 1955
<i>Discoaster adamanteus</i> Bramlette & Wilcoxon 1967	<i>Scyphosphaera apsteinii</i> Lohmann 1902
<i>Discoaster asymmetricus</i> Gartner 1969	<i>Scyphosphaera brevis</i> Varol 1984
<i>Discoaster blackstockae</i> Bukry 1973	<i>Scyphosphaera campanula</i> Deflandre 1942
<i>Discoaster bollii</i> Martini & Bramlette 1963	<i>Scyphosphaera cantharellus</i> Kamptner 1955
<i>Discoaster brouweri</i> Tan 1927 emend. Bramlette & Riedel 1954	<i>Scyphosphaera conica</i> Kamptner 1955
<i>Discoaster calcaris</i> Gartner 1967	<i>Scyphosphaera cylindrica</i> Kamptner 1955
<i>Discoaster challengerii</i> Bramlette & Riedel 1954	<i>Scyphosphaera deflandrei</i> Muller 1974
<i>Discoaster decorus</i> (Bukry) Bukry 1973	<i>Scyphosphaera expansa</i> Bukry & Percival 1971
<i>Discoaster exilis</i> Martini & Bramlette 1963	<i>Scyphosphaera gladstonensis</i> Rade 1975
<i>Discoaster intercalaris</i> Bukry 1971	<i>Scyphosphaera globulosa</i> Kamptner 1955
<i>Discoaster loeblichii</i> Bukry 1971	<i>Scyphosphaera intermedia</i> Deflandre 1942
<i>Discoaster kugleri</i> Martini & Bramlette 1963	<i>Scyphosphaera kamptneri</i> Muller 1974
<i>Discoaster neohamatus</i> Bukry & Bramlette 1969	<i>Scyphosphaera lagena</i> Kamptner 1955
<i>Discoaster neorectus</i> Bukry 1971	<i>Scyphosphaera magna</i> Kamptner 1967
<i>Discoaster pansus</i> (Bukry & Percival) Bukry 1973	<i>Scyphosphaera pacifica</i> Rade 1975
<i>Discoaster pentaradiatus</i> Tan 1927 emend. Bramlette & Riedel 1954	<i>Scyphosphaera piriformis</i> Kamptner 1955
<i>Discoaster surculus</i> Martini & Bramlette 1963	<i>Scyphosphaera procera</i> Kamptner 1955
<i>Discoaster tamalis</i> Kamptner 1967	<i>Scyphosphaera pulcherrima</i> Deflandre 1942
<i>Discoaster triradiatus</i> Tan 1927	<i>Scyphosphaera recta</i> (Deflandre) Kamptner 1955
<i>Discoaster quinquemans</i> Gartner 1969	<i>Scyphosphaera recurvata</i> Deflandre 1942
<i>Discoaster variabilis</i> Martini & Bramlette 1963	<i>Sphenolithus abies</i> Deflandre in Deflandre & Fert 1954
<i>Discosphaera tubifer</i> (Murray & Blackman) Ostenfeld 1900	<i>Sphenolithus moriformis</i> (Bronnimann & Stradner) Bramlette & Wilcoxon 1967
<i>Geminolithella rotula</i> (Kamptner) Backman 1980	<i>Sphenolithus neobabies</i> Bukry & Bramlette 1969
<i>Geminolithella subtilis</i> Varol 1989	<i>Syracosphaera? fragilis</i> Theodoridis 1984
<i>Havaster aperta</i> Theodoridis 1984	<i>Syracosphaera histrica</i> Kamptner 1941
<i>Helicosphaera carteri</i> (Wallich) Kamptner 1954	<i>Syracosphaera pulchra</i> Lohmann 1902
<i>Helicosphaera intermedia</i> Martini 1965	<i>Tetralithoides symeonidesii</i> Theodoridis 1984
<i>Helicosphaera orientalis</i> Black 1971	<i>Thoracosphaera albatrosiana</i> Kamptner 1963
<i>Helicosphaera pacifica</i> Muller & Bronnimann 1974	<i>Thoracosphaera heimi</i> (Lohmann) Kamptner 1920
<i>Helicosphaera paleocarteri</i> Theodoridis 1984	<i>Thoracosphaera saxea</i> Stradner 1961
<i>Helicosphaera stalis stalis</i> Theodoridis 1984	<i>Umbilicosphaera jafari</i> Muller 1974
<i>Helicosphaera stalis ovata</i> Theodoridis 1984	<i>Umbilicosphaera mirabilis</i> Lohmann 1902
<i>Helicosphaera sellii</i> Bukry & Bramlette 1969	<i>Umbilicosphaera sibogae</i> (Weber-van Bosse) Gaarder 1970
<i>Helicosphaera walbersdorffensis</i> Muller 1974	
<i>Hughesius gizoensis</i> Varol 1989	

Samples from each core were routinely analyzed from Holes 974B, 975B, 976B, 977A, 978A, and 979A to place zonal boundaries as accurately as possible and to determine the accurate position of bioevents (e.g., the first occurrences [FOs] and last occurrences [LOs] of stratigraphically important species). The distribution and abundance of each nannofossil species present in a sample was determined, as well as the abundance and degree of preservation of the nannofossil assemblage.

Neogene nannofossils considered in this report are listed alphabetically by generic epithet in Table 1. The relative abundance of each species (determined using a microscope magnification of 1000×) is indicated on the range charts (Tables 2–7, on the CD-ROM in the back pocket of this volume) as follows:

- A = Abundant: more than 10 specimens of a single species per field of view;
- C = Common: 1–10 specimens per field of view;
- F = Few: 1 specimen per 2–10 fields of view;
- R = Rare: 1 specimen per 11–100 fields of view;
- V = Very Rare: 1 specimen per 101–1000 fields of view; and
- B = Barren: barren of indigenous nannofossils.

Preservation of the nannofossil assemblage is indicated as follows:

- G = Good preservation: little or no evidence of dissolution and/or secondary overgrowths of calcite. Diagnostic features are fully preserved and all specimens can be identified.
- M = Moderate preservation: dissolution and/or secondary overgrowths partially alter primary morphological characteristics, but nearly all specimens can be identified to the species level.
- P = Poor preservation: Severe dissolution, fragmentation, and/or secondary overgrowths destroying primary features. Many specimens cannot be identified to the species or even generic level.

## BIOSTRATIGRAPHIC ZONATION

The irreversible nature of organic evolution produces a series of nonrepetitive “bioevents.” Geologic time, as recorded in marine sediments, is conveniently ordered by stacking these bioevents, which are usually the first occurrence (FO) or last occurrence (LO) of species, into biozones. The bioevents of planktonic organisms are most

suitable for long-range biostratigraphic correlation because, as floating organisms when alive, they had widespread geographic distribution. Biostratigraphy allows a stacking of relatively older and younger biozones, but does not give absolute ages (in years) for the biozones.

Biochronology refers to the accurate dating of the evolutionary first appearance or extinction of a species using ages calibrated by radiometric methods alone, or by interpolation between radiometrically calibrated magnetic reversals, stable isotope zones, or astronomically tuned events. These dated levels are known as first appearance datums (FADs) and last appearance datums (LADs) and they are considered to be essentially globally synchronous. The FO or LO of a species in a particular region may, however, be controlled by environmental factors and not correspond to its actual FAD or LAD. Environmental changes may cause migration of a species into or out of a region, or cause marked changes in the relative abundance of the species within the region.

The Pliocene–Pleistocene record in the Mediterranean area is a good example of a time interval and region where FOs and LOs of calcareous nannofossils do not necessarily correspond with those of extra-Mediterranean regions and where certain traditional zonal marker species may be almost absent (Rio et al., 1984; Rio et al., 1990a). These discrepancies are probably the result of the marked climatic–oceanographic changes that occurred in the Mediterranean during the Neogene. Nevertheless, Rio et al. (1990a) produced a high-resolution nannofossil biozonation based on a detailed analysis of terrestrial sections and oceanic cores. The Rio et al. (1990a) zonation is modified after the zonation of Martini (1971; Fig. 2).

The nannofossil event that most closely approximates the Pliocene/Pleistocene boundary (see next section) is the FO of *Gephyrocapsa oceanica* (>4 µm). The FO of this species also marks the MNN19A/MNN19B subzonal boundary in the Rio et al. (1990a) zonation. The boundaries of Subzone MNN18 are defined by the same bioevents that Martini (1971) used for Zone NN18, that is, the LO of *Discoaster brouweri* for the top and the LO of *D. pentaradiatus* for the base of the zone.

Martini's Zone NN17 is defined as the interval between the LO of *D. surculus* and the LO of *D. pentaradiatus*. These LO events are very closely spaced, however, and Zone NN17 is often combined, either with Zone NN18 (e.g., Siesser and Bralower, 1992) or NN16 (e.g., Rio et al., 1990a). The high sedimentation rate in the western Mediterranean allowed the separation of these two LO events in this study, and thus the recognition of a distinct Zone MNN17.

Martini's (1971) Zone NN16 is subdivided by Rio et al. (1990a) into MNN16B and MNN16A by the LO of *D. tamalis*, a distinctive event in the Mediterranean area. The LO of *Reticulofenestra pseudoumbilicus* marks the Zone NN15/NN16 boundary. Martini's (1971) Zones NN14 and NN15 were combined by Rio et al. (1990a) because of the rarity of the Zone NN14/NN15 bioevent, the LO of *Amaurolithus tricorniculatus*, in the Mediterranean region. We also found that *A. tricorniculatus* was too rare to use as a boundary marker species. Just above the level where the apparent LO of *A. tricorniculatus* does occur, however, and coincident with the last common occurrence (LCO) of *Globorotalia margaritae*, we consistently found the LCO of *Reticulofenestra pseudoumbilicus* (>7 µm). We have therefore used this nannofossil event to approximate the MNN14/MNN15 boundary. Zone MNN13 has the same top as NN13 (the FO [or FCO in the Mediterranean] of *D. asymmetricus*). The FO of *Ceratolithus rugosus* formally marks the lower boundary of Zone NN13, and the LO of *C. acutus*, a secondary marker, occurs at or near the boundary, but, again, these species occur too infrequently in the Mediterranean to be used for reliable biostratigraphy. There is not, therefore, a good nannofossil marker for the Zone NN12/NN13 boundary

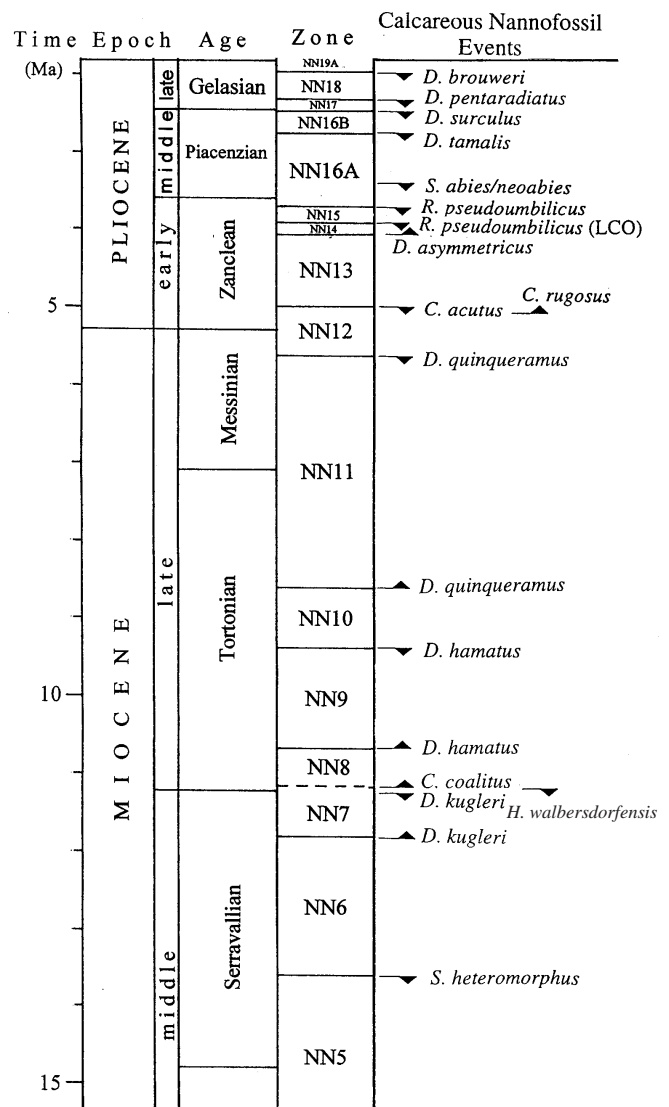


Figure 2. Neogene chronostratigraphic units and calcareous nannofossil zonation of Martini (1971). Nannofossil bioevents used to recognize zonal boundaries are shown. Time scale is from Berggren et al. (1995a).

in the study area. The last consistent occurrence (LcO) of *Helicosphaera intermedia* occurs just below the NN12/NN13 boundary in the Mediterranean and this LcO can be used for a rough approximation of the zonal boundary. In the Mediterranean region, the FO of small *Pseudoemiliana lacunosa* is also found in the upper part of Zone MNN13, and this species can be used as a secondary marker for the zone.

The Rio et al. (1990a) modifications to Martini's (1971) zonation stop with MNN12/NN12. We have subdivided Zone NN12 into Subzones NN12a, NN12b, and NN12c. Subzone NN12a is defined here as the interval from the LO of *D. quinquaramus* to the FO of *C. acutus*; Subzone NN12b is the interval from the FO of *C. acutus* to the LcO of *Helicosphaera intermedia*; Subzone NN12c is the interval from the LcO of *H. intermedia* to the LO of *C. acutus*. The total range of *D. quinquaramus* defines Zone NN11 in Martini's (1971) nannofossil zonation. This species is always very rare or absent in Mediter-

anean strata (Rio et al., 1984). We therefore recognized the approximate NN11/MNN12 boundary by using the LCO of *Helicosphaera stalis*, *H. orientalis*, *Cryptococcolithus mediaperforatus*, and *Coccolithus miopelagicus*. These species range slightly into Zone NN12, but decline markedly in numbers relative to Zone NN11. Zone NN11 can sometimes be subdivided by using the *C. pelagicus*, *Amaurolithus primus*, and *Reticulofenestra rotaria* Subzones of Theodoridis (1984). Martini's standard zonal markers were used for zoning the rest of the upper and middle Miocene. For convenience, and following the practice of Young (1991), we shall simply use "NN," rather than "MNN" for the Martini (1971) zones emended by Rio et al. (1990a; Fig. 2).

## CHRONOSTRATIGRAPHY

The approach to defining chronostratigraphic units has evolved markedly over the years. The early practice of defining a stage by use of a unit stratotype inevitably led to gaps and overlaps in time as recorded by rocks composing the stage. Current practice is to define only the boundaries between stages by an actual stratotype. The boundary is called the Global-Boundary Stratotype Section and Point (GSSP), and always defines the lower boundary of a stage (which automatically becomes the upper boundary of the underlying stage). In practice, GSSPs are located as closely as possible to traditional stage boundaries. However, priority is not a requirement in chronostratigraphy, and the most important requirement of the GSSP is that it be easily correlatable by at least one distinctive boundary event (such as a fossil marker or magnetic reversal), and preferably by several secondary markers.

The portion of the Neogene recovered during Leg 161 includes the middle Miocene Serravallian Stage, the upper Miocene Tortonian and Messinian Stages, the lower Pliocene Zanclean Stage, the middle Pliocene Piacenzian Stage, and the upper Pliocene Gelasian Stage. All these stages are stratotyped in Italy; formal GSSPs have recently been approved for the Piacenzian and Gelasian Stage boundaries (Cita et al., 1996; Cita, 1996a, 1996b).

Microfossils present in the traditional unit stratotypes have been exhaustively studied, and various schemes for correlation have been proposed. The LAD of *Sphenolithus heteromorphus* occurs just above the base of the Serravallian stratotype section, and this species (which marks the NN5/NN6 boundary) can be used to approximate the base of the stage (Rio and Fornaciari, 1994; Fornaciari et al., 1996). Rio and Fornaciari (1994) suggested that the base of the Tortonian be defined close to the FAD of the foraminifer *Neogloboquadrina acostaensis*, which occurs in the lower part of the stratotype section. The FCO of *N. acostaensis* occurs just before the FAD of *Discoaster hamatus* (the nannofossil marker for the NN8/NN9 boundary). The lower boundary of the Messinian Stage corresponds to the FAD of the foraminifer *Globorotalia conomiozea*. The nannofossil bioevent closest to this boundary is the FO of *Amaurolithus primus*.

The Miocene/Pliocene Series boundary is based on an historic event—the reflooding of the Mediterranean and the return to normal marine conditions following the Messinian salinity crisis (Benson, 1995). By this definition, no single nannofossil biochronological event occurs at this series boundary. Indeed, Benson (1995) pointed out that no one has demonstrated any global stratigraphic event that correlates with the reflooding of the Mediterranean. In this study, we approximate the Miocene/Pliocene boundary using several FOs and LOs. The boundary is in Zone NN12 below the FO of *Ceratolithus rugosus*, the LO of *C. acutus* and the LcO of *Helicosphaera intermedia*, and just above the FO of *C. acutus*.

The re-establishment of normal marine conditions also defines the base of the lower Pliocene Zanclean Stage. The disappearance of the foraminifer *Globorotalia margaritae* occurs close to the base of the Piacenzian Stage stratotype. The LO (or sometimes the LCO of *G. margaritae*) has sometimes been taken as the marker for the lower

boundary of the Piacenzian (e.g., Rio et al., 1984; Langereis and Hilgen, 1991). More recently, Rio et al. (1994) have shown the base of the Piacenzian to be at approximately the "LO" (temporary disappearance of Berggren et al. [1995b]) of *G. punctulata*. This event occurs in lower NN16A. Using nannofossils, we can therefore only approximate the lower/middle Pliocene boundary at just above the LOs of *Reticulofenestra pseudoumbilicus* (>7  $\mu\text{m}$ ) and *Sphenolithus abies/S. neoabies*.

Rio et al. (1994) proposed that the traditional two stage-two sub-series Pliocene be expanded into three units, and this proposal has recently been accepted by the IUGS (Cita, 1996a, 1996b). The Zanclean Stage remains equivalent to the lower Pliocene, but the Piacenzian is now the middle Pliocene and a new stage, the Gelasian, is the upper Pliocene. The main rationale for establishing the Gelasian is that a smaller chronostratigraphic unit (i.e., the Gelasian) can be recognized and correlated globally, thus improving stratigraphic resolution for this interval. The base of the Gelasian lies just below the NN17/NN18 boundary (Rio et al., 1994).

The Pliocene/Pleistocene boundary has long been a controversial stratigraphic topic. The location of the best stratotype section, the position of the boundary within the various sections proposed, the events to be used for correlation, and even the very concept of what the "Pleistocene" should be have been debated (e.g., see Berggren, 1971; Berggren and Van Couvering, 1974; Rio et al., 1991; Berggren et al., 1995a). International agreement seems to have been achieved at last by acceptance of the Vrica section in Calabria, Italy, as the boundary stratotype section, and designation of the top of the laminated level "e" unit within this section as the base of the Pleistocene (Aguirre and Pasini, 1985). This GSSP lies approximately at the top of the Olduvai subchron (C2n), and has been dated at 1.83 Ma (Sprovieri, 1993), or 1.81 Ma (Berggren et al., 1995a). The nannofossil marker for the Pliocene/Pleistocene boundary, the FAD of *Gephyrocapsa oceanica* (>4.0  $\mu\text{m}$ ), is slightly younger (1.75 Ma; Sprovieri, 1993) than the GSSP.

"Neogene" is a term long-used in the geological literature for the Miocene and Pliocene interval. Berggren et al. (1995a) have recently argued that the terms "Tertiary" and "Quaternary" should be discarded and replaced by "Paleogene" and "Neogene." In their treatment, the Paleogene would include the Paleocene, Eocene, and Oligocene Epochs/Series as before, but the Neogene would include the Miocene and Pliocene as well as the Pleistocene and Holocene Epochs/Series. In this study, we continue to use Neogene in its long-understood meaning—the interval comprising the Miocene and Pliocene.

## TAXONOMIC NOTES

*Reticulofenestra* spp. Species within this genus are generally distinguished on the basis of the overall size of the shields, the size of the central opening, and the width of the wall. Considerable confusion nevertheless exists in the taxonomy of the genus, with exact species concepts differing among authors. We shall not attempt to review here the often conflicting literature. The interested reader is referred to Backman (1980), Pujos (1985), Gallagher (1989), and Young (1990) for some of the more detailed examinations of this plexus. The following reticulofenestrid concepts are used in this study:

*R. rotaria*. A rare but distinctive circular form found in the late Miocene.

*R. pseudoumbilicus*. An elliptical form with a long dimension of at least 7  $\mu\text{m}$ .

*R. gelida*. A form that is also 7  $\mu\text{m}$ , but with a distinctly smaller central area than *R. pseudoumbilicus*. Gallagher (1989) considered this form to be a junior synonym of *R. pseudoumbilicus*.

*R. minuta*. Forms <3  $\mu\text{m}$  in length.

*R. minutula*. Forms 3–6  $\mu\text{m}$  in length. Some authors describe this species as ranging up to only 5  $\mu\text{m}$  in length, but this concept would leave us with the problem of what to do with the occasional 6- $\mu\text{m}$

reticulofenestrid. In the literature, these 6- $\mu$ m forms are often assigned to *R. pseudumbilicus* (e.g., Backman, 1980). Because the 7- $\mu$ m *R. pseudumbilicus* designation seems to have biostratigraphic value (Rio et al., 1990a; Young, 1990), whereas the 6- $\mu$ m forms do not, we also assigned the 6- $\mu$ m forms to *R. minutula* s.l. in Tables 2–7 (CD-ROM, back pocket, this volume).

*R. haqii*. This form has the same length as *R. minutula* s.s. (3–5  $\mu$ m). The difference between the two is the size of the central opening. *R. minutula* has a central opening >1.5  $\mu$ m, whereas *R. haqii* has an opening <1.5  $\mu$ m (Backman, 1980). We found this distinction difficult to apply consistently, and of no apparent biostratigraphic value. Pujos (1987) considered the two forms to be ecotypes of the same species; Gallagher (1989) also believed them to be synonymous. *R. minutula* is the senior synonym and is used here.

*Crenalithus* (or *Reticulofenestra*) *doronicoides*. This form has been discussed by numerous authors, with various interpretations as to the validity of the name, its taxonomic position, common usage, relationship to other species, and stratigraphic range (e.g., Backman, 1980; Matsuoka and Okada, 1989; Young, 1990). Backman (1980) considered the type specimens of *Crenalithus* (or *Reticulofenestra*) *doronicoides* to have exactly the same morphology as *R. minutula*. One does get the impression from some range charts that *R. minutula* is rather arbitrarily used in the Miocene and lower Pliocene and *C.(R.) doronicoides* in the upper Pliocene and Pleistocene for very similar specimens. In any case, Backman (1980) rejected the name “*doronicoides*” on the grounds that it could not be distinguished from one or more other legitimate species. Moreover, Young (1990) examined topotypic material which cast doubt on the very validity of the epithet “*doronicoides*”; he rejected it, considering it to be a junior synonym of *Gephyrocapsa oceanica* (forms of *G. oceanica* that have lost their bridges). We thus use *R. minutula* s.l. instead of “*C.(R.) doronicoides*” for these forms on our range charts.

*Pseudoemiliania lacunosa*. The validity of this species has received at least as much discussion in the literature as *C. (R.) doronicoides*. Matsuoka and Okada (1989) and Young (1990) provided useful reviews which we shall not repeat here. Although we have not followed Young’s (1990) change of *Pseudoemiliania* to *Reticulofenestra*, we do agree with Young (1990) and others that *P. lacunosa* has two distinct varieties: an elliptical form and a circular form. We have indicated the varieties simply as *P. lacunosa* E (= elliptical) and *P. lacunosa* C (= circular) on our range charts.

*Scyphosphaera*. This genus comprises a large number of species (53 have been named), many based on only the slightest morphological differences. The most frequently encountered species in Leg 161 holes, and elsewhere, is *S. apsteinii*. The forms that have been named *S. biarrizensis* Lezard, *S. brevis* Varol, and *S. procera* Kamptner are very similar in shape to *S. apsteinii*, and may merely represent intraspecific variation. We have, nevertheless, continued to list “squat” forms resembling *S. apsteinii* s.l. as *S. brevis*, and “slim” forms as *S. procera* on the range charts. Several specimens resembling *S. aranta* Kamptner and *S. oremesa* Kamptner were seen, but close examination showed that the lobate/domed margins (diagnostic for the definition of the species) are the result of breaking away parts of the lower margin. Siesser and Bralower (1992) reported rare specimens of these two species in Hole 762B (Exmouth Plateau). Re-examination of those specimens also shows their shape to be the result of breakage. Indeed, *S. oremesa* has never been validly reported in the literature since its erection by Kamptner (1967), and the few reports of *S. aranta* have not been confirmed.

## SITE SUMMARIES

### Site 974

Site 974 is located in the Tyrrhenian Sea on the eastern continental margin of Sardinia (Fig. 1).

Triple advanced hydraulic piston coring (APC) as deeply as possible, followed by extended core barrel (XCB) drilling to total depth,

was the strategy employed at this site to ensure recovery of a complete stratigraphic section. Voids and drilling-induced sediment disturbance can occur in APC cores. Drilling three adjacent holes increased the likelihood that any such disturbed intervals or voids in any one core could be reconciled by taking samples from the corresponding interval in one of the other holes.

### Biostratigraphy

Only one core (uppermost Pleistocene) was taken in Hole 974A. Hole 974B was cored to a depth of 208.2 mbsf; 22 cores were taken, recovering a stratigraphic sequence ranging from upper Miocene to upper Pleistocene/Holocene. In Holes 974C (22 cores; TD 199.9 mbsf) and 974D (18 cores; TD 170.5 mbsf) cores of lower Pliocene to upper Pleistocene/Holocene sediment were recovered. We examined nannofossils only in the core-catcher samples from Holes 974A, 974C, and 974D. The general biostratigraphy of these holes is summarized in the Leg 161 *Initial Reports* volume (Comas, Zahn, Klaus et al., 1996). We performed a detailed stratigraphic analysis on samples from Hole 974B.

*Hole 974B (40°21.36'N, 12°8.52'E; water depth 3454 m)*

The zonal assignment of each core is shown in Fig. 3. The distribution and relative abundance of all Neogene nannofossils identified in Hole 974B are shown in Table 2 (CD-ROM, back pocket, this volume). Neogene cores recovered from Hole 974B contain mostly abundant, well-preserved nannofossils. The only exceptions in the samples examined are in Sections 974B-22X-5 and -CC, where nannofossils are few, and preservation is moderate or poor to moderate. Reworked nannofossils make up a significant portion of the assemblage in this hole and in the other holes investigated. No hiatuses are apparent in the stratigraphic section cored.

The Pliocene/Pleistocene boundary (Subzone NN19A/NN19B boundary) is between Samples 974B-9H-4, 71–72 cm and 9H-6, 25–26 cm, based on the FO of *Gephyrocapsa oceanica* in 9H-4, 71–72 cm. We were able to use standard marker species (LO *Discoaster brouweri*, LO *D. pentaradiatus*, LO *D. surculus*, LO *D. tamalis*, LO *Reticulofenestra pseudumbilicus*) for the Pliocene zones from NN18 down to the top of Zone NN14 (Fig. 3; Table 2 [back pocket, this volume]). Because ceratoliths are so rare in these cores, we used the LCO of *R. pseudumbilicus* to approximate the NN14/NN15 boundary. The FCO of *D. asymmetricus* marks the NN13/NN14 boundary. The NN12/NN13 zonal boundary could not be determined. The top of Subzone NN12b occurs in Sample 22X-3, 123–124 cm, based on the LCO of *Helicosphaera intermedia*. The Miocene/Pliocene boundary occurs in the lower part of NN12b; in this hole the boundary would therefore be between the lowermost part of Section 974B-22X-3 and the uppermost part of 22X-5. Samples 22X-5, 18–19 cm, and 22X-CC contain *Coccolithus miopelagicus*, *Discoaster calcaris*, and a single specimen of *D. quinqueramus* (Section 974B-22X-5), which suggest a NN11 zonal assignment. We have therefore drawn the NN11/NN12 zonal boundary between Sections 974B-22X-5 and 22X-3 (Fig. 3; Table 2 [back pocket, this volume]). This position also agrees with the boundary assignment based on planktonic foraminifers (Comas, Zahn, Klaus et al., 1996).

A major lithologic change takes place in Section 974B-22X-4, at the biostratigraphically approximated Miocene/Pliocene boundary. Thin, sparsely bioturbated, red to brown, predominantly silty clay beds interspersed with sand and calcareous intervals occur from Section 974B-22X-4 downward to 22X-CC, the bottom of the hole (Comas, Zahn, Klaus, et al., 1996). Above this level the sediments are moderately to intensely burrowed nannofossil clays. This lithologic change probably marks the upward transition from a lacustrine to a normal marine environment. A lacustrine phase (the Lago Mare) is well documented as occurring in the latest Messinian in the Mediterranean region. The brackish- to freshwater lake may also have experienced brief marine incursions before the environment changed to fully marine.

HOLE 974B		
Core	Core-Section, Interval	Zone
9H	9H-4, 71-72	NN19B
10H	9H-6, 25-26	NN19A
	11H-2, 24-26	
11H	11H-3, 18-19	NN18
12H	12H-6, 24-25	
12H	12H-CC to 13H-1, 10-11	NN17
13H	13H-2, 41-42	NN16B
	13H-5, 46-47	
14H	13H-6, 18-19	NN16A
14H	14H-CC	
15H	15H-3, 30-31	NN15
15H	16H-1, 30-31	
16H	16H-2, 30 to 16H-3, 30	NN14
17X	16H-4, 30-31	
18X	22X-3, 17-18	NN13
19X		
20X		
21X		
22X		
22X	22X-3, 123-124	NN12b
	22X-5, 18-19	NN11

Figure 3. Neogene calcareous nannofossil zonation of Hole 974B. Shaded interval represents the Pliocene/Pleistocene boundary.

### Site 975

Site 975 is located in a small basin on the Menorca continental rise in the Balearic Sea (Fig. 1). As at Site 974, triple APC and double XCB cores were taken to ensure continuous sediment recovery.

#### Biostratigraphy

Only one core was taken in Hole 975A (Pleistocene; NN21A). Hole 975B (34 cores; TD 298.98 mbsf) consists of a stratigraphic sequence ranging from uppermost Miocene (NN11) to uppermost Pleistocene/Holocene (NN21B). Sediments in Hole 975C (34 cores; 307.66 mbsf) range from lower Pliocene (Zone NN12) to uppermost Pleistocene/Holocene (NN21B), and Hole 975D (16 cores; TD

157.03 mbsf) from upper Pliocene (NN17) to uppermost Pleistocene/Holocene (NN21B). The biostratigraphy of Holes 975A, 975C, and 975D is based on core-catcher samples only, and is reported in the Leg 161 *Initial Reports* volume. We performed a detailed stratigraphic analysis on samples from Hole 975B.

*Hole 975B (38°53.79'N, 4°30.60'E; water depth 2416 m)*

Figure 4 shows the zonal assignment of each core. Table 3 (CD-ROM, back pocket, this volume) gives the distribution and relative abundance of the nannofossil assemblage in Hole 975B.

Neogene nannofossils are common to abundant and mostly well preserved in samples from this hole, except in the lowermost sample collected (161-975B-34X-CC), where nannofossils are few and poorly preserved. We found no hiatuses in the section cored.

Sample 161-975B-13H-CC contains the FO of *G. oceanica* and thus marks the Pliocene/Pleistocene boundary (Subzones NN19A/NN19B boundary). We used the same biozonal markers as in Hole 974B in this hole from Zone NN18 down to Zone NN13. Again, the NN12/NN13 zonal boundary could not be determined. Recognition of the Zones NN11/NN12 boundary also presented a problem. Lithologically, the open-marine lower Pliocene sediments end rather abruptly downhole in Zone NN12 in Section 975B-33X-2. A thin unit of laminated, possibly intertidal, calcareous silty clay occurs from 975B-33X-2, 131 cm, down to 33X-CC, underlain by gypsum and gypsiferous chalk to the bottom of the hole (Comas, Zahn, Klaus, et al., 1996). Nannofossils suggestive of the upper Miocene (*Cryptococcolithus mediaperforatus*, *Helicosphaera stalis stalis*, *H.s. ovata*, *H. orientalis*, and *Coccolithus miopelagicus*) occur in the intertidal calcareous clays in Section 975B-33X-CC in what is apparently a marine intercalation within the gypsum. We have therefore drawn the NN11/NN12 zonal boundary (which approximates the Miocene/Pliocene boundary here) between 975B-33X-CC and 33X-3, 130–131 cm. Sample 975B-33X-3, 130–131 cm, lacks the Miocene markers found below and contains nannofossils typical of Zone NN12 (Table 3, back pocket, this volume). We believe normal open-ocean conditions were re-established by this time. Planktonic foraminifers are all dwarfs below 975B-33X-3, 80–82 cm, and one benthic foraminifer found in 33X-CC is characteristic of a brackish-water environment such as the Lago Mare (Comas, Zahn, Klaus, et al., 1996).

### Site 976

Site 976 is located in the Alboran Sea, about 60 km off southern Spain and about 110 km east of the Strait of Gibraltar (Fig. 1). Site 976 is about 8 km northeast of DSDP Site 121.

#### Biostratigraphy

Recovery at Hole 976A consisted of one core (Pleistocene/Holocene; NN21B). Hole 976B was dedicated to tectonic objectives. In this hole we APC- and XCB-cored continuously to a depth of 928.7 mbsf, penetrating 660.2 m of a sedimentary sequence (72 cores) ranging from middle Miocene (Serravallian; NN7) to uppermost Pleistocene/Holocene (NN21B), and RCB-cored 268.5 m into pre-middle Miocene metamorphic rocks dominated by gneiss and schist (34 cores). Hole 976C was cored continuously from the uppermost Pleistocene/Holocene (NN21B) to the uppermost Pliocene (NN19A). Four cores were taken in Hole 976D; all were in the upper Pleistocene/Holocene (NN21A–NN21B). Hole 976E was washed down to the lower Pliocene (NN12) at 534.8 mbsf, then RCB cored to the middle Miocene (28 cores). The general biostratigraphy for all five holes, based on core-catcher samples, is given in the Leg 161 *Initial Reports* volume. The detailed biostratigraphy of Hole 976B is given below.

*Hole 976B (36°12.3'N, 4°18.8'W; water depth 1108 m)*

Figure 5 shows the zonal assignment of each core. Distribution and abundance of all species identified in Hole 976B are given in Table 4 (CD-ROM, back pocket, this volume).

HOLE 975B		
Core	Core-Section, Interval	Zone
13H	13H-CC	NN19B
14H	14H-2, 75-77 15H-3, 81-82	NN19A
15H	15H-5, 101-103	NN18
16H	17H-CC	
17X		
18X	18X-1, 20-21	NN17
19X	20X-CC	
20X		
21X	21X-1, 29-30 21X-3, 30-31	NN16A
22X	23X-4, 15-16	
23X		
24X	23X-5, 14-15	NN15
25X	25X-6, 19-20	
26X	25X-CC to 26X-CC	
27X	27X-1, 24-25	NN13
28X		
29X		
30X	33X-3, 130-131	NN12
31X		
32X		
33X	33X-3, 130-131	NN11
34X	33X-CC	

Figure 4. Neogene calcareous nannofossil zonation of Hole 975B. Shaded interval represents the Pliocene/Pleistocene boundary.

Cores recovered from Hole 976B contain common to abundant Neogene nannofossils except for intervals from 161-976B-39X-CC to 44X-2, 20–21 cm, from 47X-3, 21–22 cm, to 48X-CC, from 72X-CC to 73X-1, 0–4 cm, and 75R-1, 16–17 cm. Nannofossils are mostly rare to few in these intervals, and two samples (976B-42X-CC and 72X-3, 21–22 cm) are barren. Preservation ranges from moderate to good except in samples taken from Cores 976B-72X, 73X, and 74X, in which preservation is poor. Hiatuses occur in the stratigraphic section, as described below.

The NN19A/NN19B Subzone boundary (Pliocene/Pleistocene boundary) is between Samples 976B-38X-CC and 39X-3, 22–23 cm. The NN18/NN19A zonal boundary is marked by the LO of *D. brou-*

HOLE 976B		
Core	Core-Section, Interval	Zone
38X	38X-CC	NN19B
39X	39X-3, 22-23	NN19A
40X		
41X		
42X		
43X		
44X		
45X		
46X		
47X		
48X		
49X	49X-CC	NN18
50X		
51X		
52X		
53X		
54X	55X-CC	
55X		
56X		
57X	61X-7, 71-73	NN12
58X		
59X		
60X		
61X		
62X	61X-CC	NN11
63X		
64X		
65X		
66X		
67X		
68X	69X-1, 21-22	NN8
69X		
70X		
71X	71X-3, 21-22	NN7
72X	71X-4, 21-22	
73X		
74X		
75R		

Figure 5. Neogene calcareous nannofossil zonation of Hole 976B. Shaded interval represents the Pliocene/Pleistocene boundary. Vertically lined intervals indicate hiatuses.

*veri* in Sample 49X-CC (Fig. 5; Table 4 [CD-ROM, back pocket, this volume]). Samples from 976B-49X-CC down to 55X-CC contain a normal, moderately to well-preserved Zone NN18 assemblage. This interval lacks *D. pentaradiatus*, *D. surculus*, and *D. tamalis*, the marker species for Zones NN17 and NN16 (a single specimen, probably reworked, of *D. pentaradiatus* was found in 52X-CC). The next underlying sample, 976B-56X-1, 18–19 cm, contains *D. pentaradia-*

tus, plus *R. pseudoumbilicus* (common) and *Sphenolithus abies*, but lacks *P. lacunosa* and *H. sellii*. The presence of *R. pseudoumbilicus* and *S. abies*, which range no higher than Zone NN15, and the absence of *P. lacunosa* and *H. sellii*, which first appear in NN13 (FcO of *H. sellii*) and range into Zone NN19 indicate Section 976B-56X-1 is in Zone NN12. A hiatus therefore exists between Samples 56X-1, 18–19 cm and 55X-CC, spanning at least Zones NN13 to NN17. Using the time scale in Figure 2, we estimate the duration of this hiatus in the Mediterranean to be at least 2.5 m.y.

The NN11/NN12 (approximate Miocene/Pliocene) zonal boundary is between Samples 976B-61X-7, 71–73 and 61X-CC, based on the LO of *Cryptococcolithus mediaperforatus*, *Reticulofenestra rotaria*, and *Coccolithus miopelagicus* in 61X-CC. Sample 976B-68X-CC contains *Reticulofenestra rotaria* and *Amaurolithus primus*, indicating Zone NN11. *Discoaster pentaradiatus* also occurs in this sample. *R. rotaria* and *A. primus* first appear in Zone NN11, and *D. pentaradiatus* first appears in NN9. Sample 976B-69X-1, 21–22 cm and lower samples lack all three of these species, suggesting a zonal assignment below NN9. *D. kugleri* has its LO in Sample 976B-71X-4, 21–22 cm. In the absence of *Catinaster coalitus*, which is not found in the Mediterranean (Rio et al., 1990a), we consider the LO of *D. kugleri* to approximate the upper boundary of Zone NN7. We therefore assign intervening samples from 976B-71X-3, 21–22 cm to 69X-1, 21–22 cm to Zone NN8. The missing Zones NN9 and NN10 represent a hiatus of at least 2.0 m.y. (Fig. 2). The sporadic co-occurrence of *H. walbersdorfensis*, *D. kugleri*, and *Calcidiscus macintyreii* in the interval from 976B-71X-4, 21–22 cm, to 75R-2, 67–69 cm, indicates that these lowermost cores are still in Zone NN7.

Sediments at the top of Core 976B-75R-1 contain downhole contamination. Scrapings of calcareous material from pebbles in Samples 976B-80X-1, 22 cm, and 80X-1, 124 cm, yielded rare nannofossils that could only be assigned a Miocene age.

### Site 977

Site 977 is located in the eastern Alboran Sea, midway between Spain and Algeria (Fig. 1). The drilling site was spudded in a sediment-filled graben bounded by the Maimonides Ridge to the north and the Yusuf Ridge to the south. The Al-Mansour Seamount lies in the center of the graben, dividing it into two east-west-trending basins. Site 977 is on the south side of Al-Mansour (Fig. 1). Only one hole was drilled at this site during Leg 161 (Hole 977A).

### Biostratigraphy

Hole 977A (36°01.9'N, 1°57.3'W; water depth 1984 m)

This hole was APC- and XCB-cored continuously to 588.9 mbsf; 62 cores were recovered. An attempt to drill deeper after a bit change failed and the hole was abandoned.

The stratigraphic interval recovered ranges from middle/upper Miocene (NN7–NN11) to uppermost Pleistocene/Holocene (NN21B). Figure 6 shows the zonal assignment of each core. Table 5 (CD-ROM, back pocket, this volume) gives the abundance and distribution of all species identified in the cores.

Cores recovered from Hole 977A contain common to abundant Neogene nannofossils except for Samples 161-977A-60X-1 (Piece 1) and 60X-CC, which contain few nannofossils. Preservation is good, or moderate to good, in all cores except in the lower Pliocene interval from Samples 977A-56X-CC to 60X-CC, where preservation is moderate or poor.

*Gephyrocapsa oceanica* makes its FO in Sample 161-977A-29X-1, 65–67 cm, establishing the Subzone NN19A/NN19B (Pliocene/Pleistocene) boundary between Sample 29X-1, 65–67 cm, and Sample 29X-2, 65–67 cm. We recognized the boundaries of Zones NN18, NN17, NN16B, NN16A, NN15, and NN14 using the species markers noted for Holes 974B, 975B, and 976B. A brief hiatus occurs be-

HOLE 977A		
Core	Core-Section, Interval	Zone
28X	29X-1, 65-67	NN19B
29X	29X-2, 65-67	NN19A
30X		
31X		
32X		
33X		
34X	34X-1, 16-17	NN18
35X		
36X		
37X		
38X	40X-4, 148-150	
39X		
40X	40X-5, 18 to 41X-1, 24	
41X	41X-2, 23-24	NN16B
42X		
43X	44X-CC	
44X	45X-1, 20-21	NN16A
45X		
46X	47X-3, 20-21	NN15
47X	47X-5, 21-22	
48X	51X-2, 21-22	
49X		
50X	51X-3, 18-19	NN14
51X		
52X	52X-6, 19	NN13
53X	52X-6, 23	
54X	54X-3, 82-84	
55X	54X-5, 89-91	NN12b
56X		
57X	57X-CC	
58X	60X-1, pc.1	NN11   NN7
59X		
60X		
61X		
62X		
63X		

Figure 6. Neogene calcareous nannofossil zonation of Hole 977A. Shaded interval represents the Pliocene/Pleistocene boundary. Vertically lined interval indicates a hiatus.

tween Samples 52X-6, 19 cm, which contains *P. lacunosa* and *H. sellii*, and Sample 52X-6, 23 cm, which lacks these species. The hiatus probably represents the uppermost part of Zone NN13, and perhaps the lower part of Zone NN14. The duration of this hiatus is difficult to estimate, but probably lasted less than 1.0 m.y. (Fig. 2). The stratigraphic interval from 977A-54X-5, 89–91 cm, to 57X-CC contains *H. intermedia* and lacks upper Miocene forms. We assign this interval to Zone NN12b. Poor recovery from Core 58X to 59X pre-

cludes zoning of this interval. Scrapings from the calcareous matrix surrounding pebbles in Samples 977A-60X-1 (Pieces 1, 4) yielded an assemblage containing the Miocene forms *H.s. stalis*, *C. miopelagicus*, and *Cyclicargolithus floridanus* (Table 5 on CD-ROM, back pocket, this volume), indicating Zones NN7–NN11. The pebbles probably represent a sedimentary gravel unit resulting from erosion caused by the post-Messinian flooding of the western Mediterranean (Tribble et al., 1995). The gravel unit corresponds to the “M” seismic reflector at the Miocene/Pliocene boundary.

### Site 978

Failing our attempt to drill deeper at Site 977, we moved 24 km to the north and spudded Site 978 in the basin on the north side of the Al-Mansour Seamount (Fig. 1).

#### Biostratigraphy

Hole 978A (36°13.9'N, 2°03.4'W; water depth 1942 m)

Rotary coring was intermittent in this single Site 978 hole until 213.0 mbsf, after which coring was continuous to a depth of 694.3 mbsf; 53 cores were recovered. A free-fall funnel (FFF) was then dropped and the bit changed in order to drill deeper in this hole. However, after lowering the new bit, the hole could not be relocated (apparently because the FFF shifted when the old bit was withdrawn), and the site was abandoned.

The sedimentary sequence recovered ranges from upper Miocene Zone NN11 to upper Pleistocene (Zone NN19F). Zonal assignments for each core are shown in Figure 7; abundance and distribution of all nannofossil species are given in Table 6 (CD-ROM, back pocket, this volume).

Most Neogene samples obtained from Hole 978A contain common to abundant nannofossils, except for intervals in Cores 161-978A-49R, 51R, 52R, and 53R in which nannofossils are “rare” or “few” (Table 6 on CD-ROM, back pocket, this volume). Nannofossil preservation is moderate to good in all samples except 46R-CC, where preservation is poor to moderate.

Coring was intermittent down to 213.0 mbsf (lower Pleistocene), after which coring was continuous. The Subzone NN19A/NN19B (Pliocene/Pleistocene) boundary is between Samples 161-978A-4R-1, 6–8 cm, and 4R-1, 64–66 cm. The presence of the usual marker species shows that all Pliocene zones are present (Table 6 on CD-ROM, back pocket, this volume), with the NN12/NN13 boundary subject to the usual uncertainty. The LOs of *H. s. stalis*, *H. s. ovata*, *H. orientalis*, *R. rotaria*, *C. miopelagicus*, and *C. mediaperforatus* occur in a stepwise fashion from 978A-47R-CC to 45R-CC. We have tentatively placed the NN11/NN12 zonal boundary at the last co-occurrence of *H. s. ovata*, *H. orientalis*, and *C. miopelagicus* in 978A-47R-CC (Fig. 7). The highest upcore occurrence of upper Miocene planktonic foraminifers is also in Core 47R, and the same gravel bed found at the top of the Messinian in Hole 977A occurs in this hole from Sample 978A-46R-1, 0 cm, to 47R-1, 7 cm (Comas, Zahn, Klaus, et al., 1996). Sections 978A-48R-1 through 53R-CC contain low numbers of upper Miocene nannofossils consistent with Zone NN11. *Reticulofenestra rotaria* is present between 978A-49R-3 and 50-2, suggesting the presence of the *R. rotaria* Subzone of Theodoridis (1984). *Cyclicargolithus floridanus* also occurs rarely throughout this interval, but based on the specimens' rarity and preservation state, we consider them to be reworked. Reworked Cretaceous and Paleogene nannofossils are present in greater than usual numbers from Sample 45R-CC downward to the bottom of the hole.

### Site 979

Site 979 is located in the southern Alboran Sea, at the base of the southern flank of the Alboran Ridge (Fig. 1).

HOLE 978A		
Core	Core-Section, Interval	Zone
3R	4R-1, 6-8	NN19B
4R	4R-1, 64-66	NN19A
5R		
6R		
7R		
8R		
9R		
10R	11R-4, 19-20	NN18
11R		
12R		
13R	11R-5, 20-21	NN18
14R		
15R	15R-1, 20-21	NN17
16R	15R-2, 18-19	
17R	15R-3, 20-21	NN16B
18R	20R-1, 20-21	
19R		
20R	20R-3, 20-21	
21R		
22R	28R-2, 20-21	NN16A
23R		
24R		
25R		
26R		
27R		
28R	28R-3, 20 to 29R-2, 19	NN15
29R	29R-3, 19-20 31R-2, 20-21	NN14
30R		
31R	31R-3, 20-21	NN13
32R		
33R	34R-CC	NN12
34R		
35R	35R-3, 7-8	NN12
36R		
37R		
38R		
39R		
40R		
41R	46R-CC	NN11
42R		
43R		
44R		
45R	47R-CC	NN11
46R		
47R		
48R		
49R		
50R		
51R		
52R		
53R		

Figure 7. Neogene calcareous nannofossil zonation of Hole 978A. Shaded interval represents the Pliocene/Pleistocene boundary.

**Biostratigraphy**

Hole 979A (35°43'N, 3°12.35'W; water depth 1062 m)

This, the only hole drilled at this site, was APC- and XCB-cored to a depth of 583.14 mbsf; 62 cores were recovered. The sedimentary sequence recovered ranges from middle Pliocene (Zone NN16A) to upper Pleistocene/Holocene (Zone NN21B). Zonal assignments for each core are shown in Figure 8; abundance and distribution of all species are given in Table 7 (CD-ROM, back pocket, this volume).

Neogene samples obtained from Hole 979A contain common to abundant nannofossils, except for Sample 161-979A-50X-CC, in which nannofossils are rare. Preservation ranges from moderate to good. The Subzone NN19A/NN19B (Pliocene/Pleistocene) boundary in this hole occurs between Samples 979A-37X-CC and 38X-3, 20–21 cm. All Pliocene zones from NN18 to NN16A are present, based on recognition of the same marker species used in the previous holes. The hole terminated in Zone NN16A.

A brief NN17 intrazonal hiatus is inferred between 979A-51X-CC and 52X-3, 15–16 cm, based on the LO and co-occurrence of the foraminifer *Globorotalia bononiensis* and the nannofossil *D. pentaradiatus* at the same level (476.41 mbsf). Normally the LAD of *D. pentaradiatus* slightly predates the LAD of *G. bononiensis* (by about 0.1 m.y.). No other microfossil change is apparent at this level, and no changes in lithology were noted for this level by the shipboard sedimentologists (Comas, Zahn, Klaus, et al., 1996).

**PALEOCLIMATOLOGY**

The Pliocene was a time when global climatic conditions were in full decline, changing from the Greenhouse Earth of the early Tertiary to the Icehouse Earth of the late Neogene and Quaternary. Climatic change has a direct effect on the temperature of oceanic surface waters. Many different proxies have been used to assess the changing temperature of oceanic waters, and thus climate, with time (e.g., oxygen isotope ratios, alkenone measurements, temperature-sensitive single species or assemblages of various microfossils, structural changes in microfossil skeletons, and so on). In this study, we have used a technique employing two temperature-diagnostic nannofossil species in an attempt to identify trends in surface-water temperature changes in the western Mediterranean during the Pliocene.

Calcareous nanoplankton are organisms that live in the upper surface waters of the oceans and are thus directly influenced by surface-water changes. The discoaster group has long been known to prefer warm waters, and several earlier workers have produced paleotemperature studies using the ratio of warm-water discoasters, as a group, to cool-water *Chiasmolithus* or *Coccolithus* (e.g., Bukry, 1978, 1981; Haq et al., 1977; Siesser, 1980, 1984; Raffi and Rio, 1981). In the Neogene, however, several discoasters (*D. variabilis*, *D. intercalaris*, *D. tamalis*, and *D. asymmetricus*) are believed to have preferred cool waters (Bukry, 1981; Rio et al., 1990a). A single discoaster species, *Discoaster brouweri*, which has a well-established preference for warm waters (e.g., Bukry, 1978, 1981; Siesser, 1975; Muller, 1985; Wei et al., 1988), was thus selected as the warm-water proxy for this study.

*Coccolithus pelagicus* was chosen as the cool-water proxy. *Coccolithus pelagicus* lives only in cold-temperate (6°–14°C) northern hemisphere waters today (Mcintyre et al., 1970; Raffi and Rio, 1981), but has apparently changed its habitat with time. In Miocene and earlier Tertiary sediments, *C. pelagicus* was common in tropical environments as well as in cooler waters (Bukry, 1981). Bukry (1981) made a careful analysis of the distribution of this species, concluding that by the Pliocene *C. pelagicus* had evolved an affinity for cool water that made it an effective proxy for determining paleotemperature trends. Raffi and Rio (1981) also concluded that *C. pelagicus* was a

HOLE 979A		
Core	Core-Section, Interval	Zone
37X	37X-CC	NN19B
38X	38X-3, 20-21	NN19A
39X		
40X		
41X		
42X	45X-2, 20-21	NN19A
43X		
44X		
45X	45X-3, 20-21	NN18
46X		
47X		
48X		
49X	52X-2, 21-22	NN18
50X		
51X		
52X	52X-3, 15 to 53X-2, 22	NN17
53X	53X-3, 23-24	NN16B
54X		
55X		
56X	56X-CC	NN16A
57X	57X-3, 21-22	
58X		
59X		
60X		
61X		
62X		

Figure 8. Neogene calcareous nannofossil zonation of Hole 979A. Shaded interval represents the Pliocene/Pleistocene boundary.

good paleotemperature indicator for the Mediterranean during the late Pliocene.

*Discoaster brouweri* and *C. pelagicus* have additional advantages in that they are both normally significant components of nannofossil assemblages, and they are also less affected by diagenetic changes than many other species. The changing downhole ratio of these two nannofossil species should, therefore, be a good paleotemperature indicator, reflecting gross changes in water temperature with time. Using a ratio rather than absolute abundances of the two species avoids potential error caused by variations in the density of specimens sedimented on a slide. Wei et al. (1988) also used the ratio of these two species to investigate Neogene water temperatures on the Galicia Margin.

In this study, we counted 100 specimens of *D. brouweri* and *C. pelagicus* along random traverses across slides from each Leg 161 Pliocene core. We included all varieties of "*D. brouweri*" in our count of *D. brouweri* s.l.: *D. brouweri* var. *rutellus* Gartner; *D. brouweri* subsp. *bipartitus* Haq and Berggren; *D. brouweri* subsp. *brouweri* Theodoridis; *D. brouweri* subsp. *streptus* Theodoridis, and *D. tri-radiatus* Tan. Species counts for each sample examined are shown in the Appendix. Results are expressed as the percentage of *D. brouweri*

in the total count of 100 *D. brouweri* and *C. pelagicus* specimens, and are plotted against nannofossil zones in Figures 9–11.

**Hole 974B**

The *D. brouweri*-*C. pelagicus* ratio is generally low in the early part of Zone NN12, suggesting cool waters (Fig. 9). In early Zone NN13 waters warmed considerably, before becoming cool again in late NN13. Temperatures began to rise in Zone NN14 and continued

to be relatively high throughout the NN14–NN17 interval. Zones NN16A, NN16B, and NN17 show a major warming trend, with a sample in NN16B (974B-13H-3, 27–28) showing the highest ratio measured in any Leg 161 hole (*D. brouweri* = 47; *C. pelagicus* = 53). Zone NN18 shows decidedly cool waters. Raffi and Rio (1981) used the abundance of *C. pelagicus* and discoasters (as a group) to estimate relative temperatures for the Pliocene at DSDP Site 132. The data presented in our study only partially agree with the data presented by Raffi and Rio (1981). This may be because different proxies were

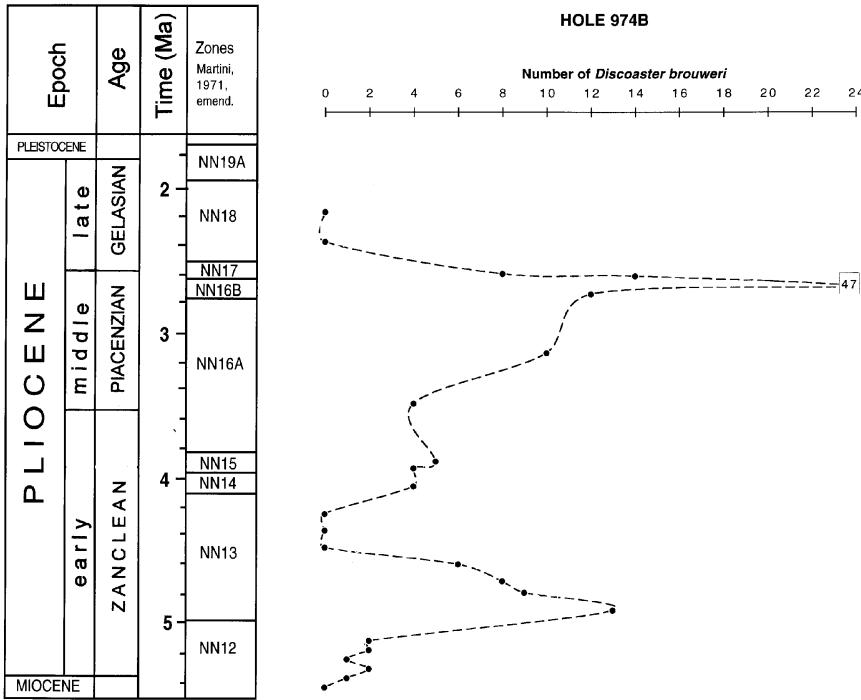


Figure 9. Relative changes in Pliocene surface-water temperatures in Hole 974B, based on the ratio of *Discoaster brouweri* (warm water) to *Coccolithus pelagicus* (cool water).

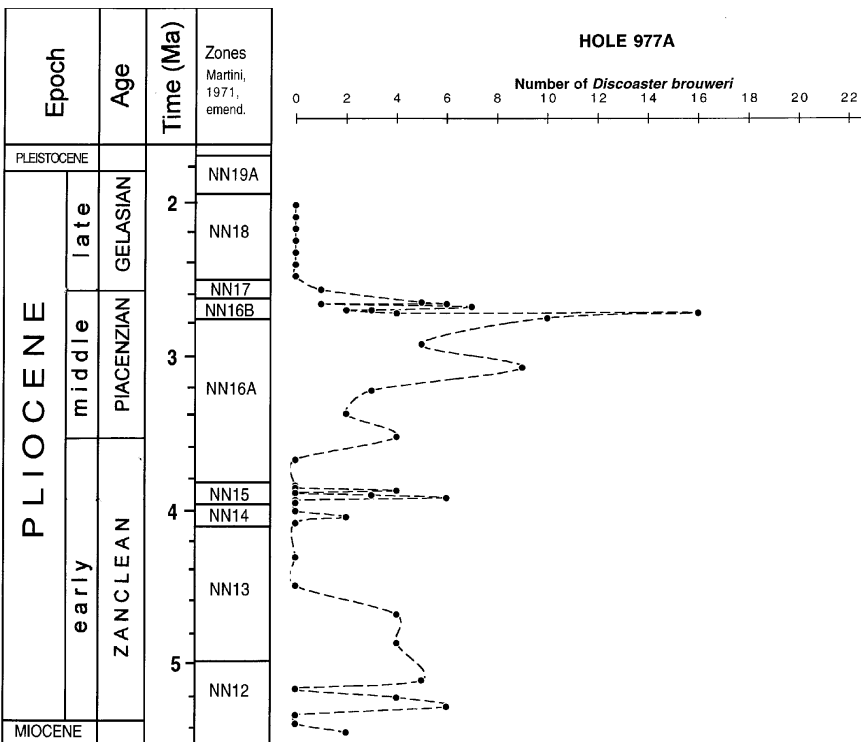


Figure 10. Relative changes in Pliocene surface-water temperatures in Hole 977A, based on the ratio of *D. brouweri* to *C. pelagicus*.

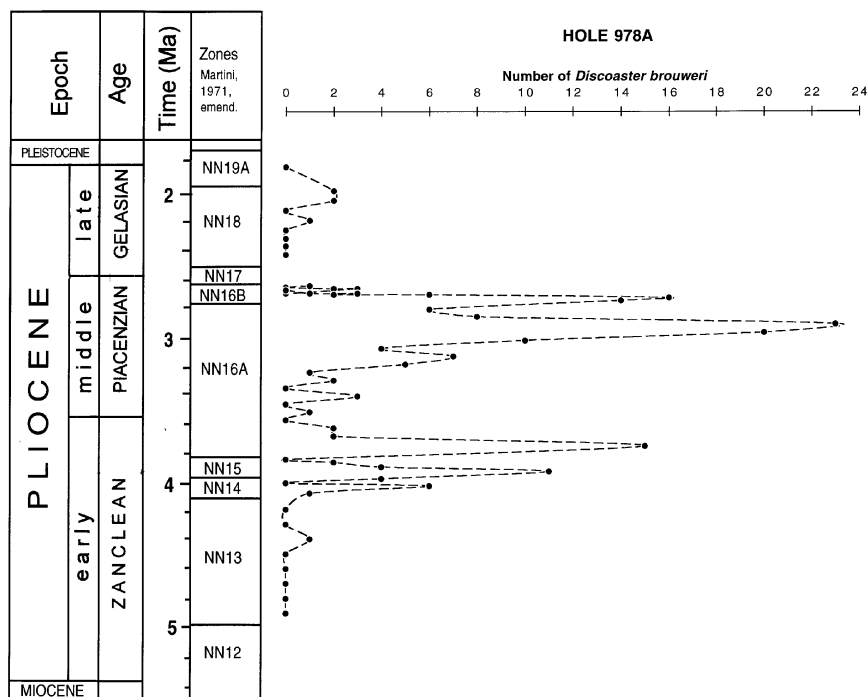


Figure 11. Relative changes in Pliocene surface-water temperatures in Hole 978A, based on the ratio of *D. brouweri* to *C. pelagicus*.

used, as well as zonations differing in their degree of resolution, making close comparison difficult. The marked increase in discoasters/*D. brouweri* during the late Pliocene followed by the precipitous reduction of these forms in Zone NN18 is, however, common to both studies.

We believe the sharp warm peak centered on Zone NN16B is the mid-Pliocene warm interval described in several recent papers (e.g., Crowley, 1996; Dowsett et al., 1996).

#### Hole 975B

The *D. brouweri* values in this hole fluctuate erratically, and lack clear trends (see Appendix; Fig. 4). The largest warm-water peaks are in early Zone NN13, late NN15–early NN16A, and NN17.

#### Hole 976B

Zones NN13 to NN17 are missing in this section. Ratios in the remaining intervals show a marked warm-water peak in latest Zone NN12, with cool waters in Zone NN18 (see Appendix; Fig. 5).

#### Hole 977A

A brief cool-water interval in early Zone NN12 was followed by generally warm waters from the middle of NN12 into early Zone NN13 (Fig. 10). Waters were cool in late Zones NN13 and NN14, with warming occurring briefly again in Zone NN15, followed by a brief cooling in late NN15–early NN16A. A period of sustained warming followed which peaked in Zone NN16B. The brief, but markedly warm period in earliest NN16B is the mid Pliocene warm interval (Crowley, 1996; Dowsett et al., 1996). Waters cooled in Zones NN17 and NN18.

#### Hole 978A

This hole contains the most expanded stratigraphic section obtained during Leg 161 (Fig. 11). Cool waters in Zone NN13 were followed by fluctuating cool and warm intervals in NN14 and NN15. Sustained warming began in late Zone NN16A and continued into NN16B. The warmest waters of the Pliocene occurred in the middle

Pliocene (late NN16A–NN16B). Waters began to cool significantly in late NN16B, a trend that continued into Zones NN17 and NN18.

#### Hole 979A

This section ranges only from Zones NN16A to NN18. Warm waters in early Zone NN16A became cooler in late Zone NN16A. Alternately warm- and cool-water peaks fluctuate erratically and closely in time in Zone NN16B, although this zone is overall the warmest interval of the Pliocene at this site (Appendix; Fig. 8). Zones NN17 and NN18 were cool-water intervals.

## SYNTHESIS

The ratio/temperature variations in different zonal intervals among the holes (Figs. 9–11; Appendix) require examination. In the foregoing description of each hole, we took the conventional approach of assuming that fluctuating ratios were caused entirely by changing surface-water temperatures. It is possible, however, that although surface-water temperatures are controlling the overall long-term trends, regional variation is being overprinted by the short-term trends of other, unknown influences (nutrient supply? salinity? turbidity?). This may explain the variation in ratio patterns seen among widely separated holes from the Tyrrhenian, Balearic, and Alboran Seas.

Several overall trends do emerge from the data. All holes show a dramatic reduction in *D. brouweri* beginning at least by the early part of Zone NN18. This might be interpreted simply as the declining abundance of a taxon nearing its extinction (at the end of Zone NN18). In most temperate to subtropical sites, however, *D. brouweri* occurs in significant numbers throughout Zone NN18, and we believe cooling waters were the true cause of this marked decline in abundance in Zone NN18 in the Mediterranean. Evidence for the timing of the onset of Northern Hemisphere glaciation (between 2.8 and 2.5 Ma) has been summarized by King (1996). The lower boundary of Zone NN18 occurs at about 2.5 Ma (Fig. 2). Wei et al. (1988) also found that the *D. brouweri*-*C. pelagicus* ratio decreased sharply after about 2.5 Ma on the Galicia Margin. Another predominantly cool-water interval also occurs in Zone NN13 in Leg 161 holes.

Rio et al. (1990b) presented a paleoclimatic synthesis of ODP Site 653 (Tyrrhenian Sea) based on micropaleontologic and oxygen isotope data. They also found that a major cooling began at 2.4 Ma (using a different time scale). Their dates for cool-water intervals in the early Pliocene (estimated to be in Zones NN14–NN15) are somewhat later than the corresponding interval suggested here (late Zone NN13). Their time scale is presented in terms of years, rather than biozones, and at least part of the discrepancy may result from the different scales used to date the intervals. Rio et al. (1990b) identified cooling at about 3.1 Ma (which on our scale would be in Subzone NN16A), based on an increase in cool-water *C. pelagicus*. We also found an overall increase in *C. pelagicus* abundance during this interval, but a correspondingly much larger increase in warm-water *D. brouweri*, which suggests a time of generally warm waters in late Subzone NN16A. Overall warm-water intervals occur in most holes in late Zone NN12–early NN13 and in Zones NN15, NN16A, and NN16B.

The warmest surface waters in the Mediterranean during the Pliocene occur during a brief interval centered on Zone NN16B. This “warmest” peak was found at Sites 974B, 977A, 978A, and 979A; a warm peak also occurs in Subzone NN16B at Site 975B, although not the warmest interval at that site. Zones NN13 to NN17 are missing at Site 976B. In several holes, this time of warm waters began in late Zone NN16A and extended into Zone NN17, but the peak warm period is in the middle Pliocene from Subzones NN16A to latest NN16B (about 3.0 to 2.6 Ma).

Crowley (1996), Dowsett et al. (1996), Raymo et al. (1996), and others have stated that the mid-Pliocene was the last time when global average temperatures were greater than temperatures of today. The time of this warm period is estimated to be around 3.0 Ma (Raymo et al., 1996). Crowley (1996) and Raymo et al. (1996) suggested that this Pliocene warmth may have been caused by higher atmospheric CO<sub>2</sub> levels, quoting data showing that mid-Pliocene CO<sub>2</sub> levels were about 98–100 ppm higher than today’s levels, or by increased oceanic heat transport. Whatever the cause of the mid-Pliocene climatic peak, data from the Mediterranean presented here provide supporting evidence for the warm interval and further constrain the time of its occurrence.

## SUMMARY

We investigated one site in the Tyrrhenian Sea, one in the Balearic Sea, and four in the Alboran Sea during Leg 161. Neogene nannofossils are generally abundant and mostly well preserved at all sites. The following Neogene sections were recovered: a complete upper Miocene (Zone NN11) to uppermost Pliocene (Zone NN19B) sequence in Holes 974B and 975B; middle Miocene (Zone NN7) to uppermost Pliocene in Hole 976B; middle or upper Miocene (Zones NN7–NN11) to uppermost Pliocene in Hole 977A; middle Miocene (Zone NN11) to uppermost Pliocene in Hole 978A; and middle Pliocene (Zone NN16A) to uppermost Pliocene in Hole 979A. Several hiatuses exist in the upper Miocene and Pliocene in Holes 976B, 977A, and 979A.

The changing downhole ratio of cool-water *Coccolithus pelagicus* to warm-water *Discoaster brouweri* indicates a relatively cool period during the early part of Zone NN12, a warm period during later NN12–early NN13, and another cool period during late NN13. Generally warm conditions prevailed during Zones NN15, NN16A, and NN16B, with the warmest waters of the Pliocene occurring in Zone NN16B. A dramatic cooling began by Zone NN18.

## ACKNOWLEDGMENTS

This work was supported by a grant to W. G. Siesser from the JOI/U.S. Science Support Program. We thank Messrs. Nick Lillios, John

Marler, Christophe Popper, and Kurt Vanderyt for their able laboratory assistance during various stages of the project.

## REFERENCES

- Aguirre, E., and Pasini, G., 1985. The Pliocene-Pleistocene boundary. *Episodes*, 8:11–120.
- Backman, J., 1980. Miocene-Pliocene nannofossils and sedimentation rates in the Hatton-Rockall Basin, NE Atlantic Ocean. *Stockholm Contrib. Geol.*, 36:1–91.
- Benson, R.H., 1995. Editorial: Is the death of an ocean falling through a stratigraphic crack? *Paleoceanography*, 10:1–3.
- Berggren, W.A., 1971. Tertiary boundaries and correlations. In Funnell, R.M.S., and Riedel, W.R. (Eds.), *The Micropalaeontology of Oceans*: (Cambridge) Cambridge Univ. Press, 693–809.
- Berggren, W.A., Hilgen, F.J., Langereis, C.G., Kent, D.V., Obradovich, J.D., Raffi, I., Raymo, M.E., and Shackleton, N.J., 1995a. Late Neogene chronology: new perspectives in high-resolution stratigraphy. *Geol. Soc. Am. Bull.*, 107:1272–1287.
- Berggren, W.A., Kent, D.V., Swisher, C.C., III, and Aubry, M.-P., 1995b. A revised Cenozoic geochronology and chronostratigraphy. In Berggren, W.A., Kent, D.V., Aubry, M.-P., and Hardenbol, J. (Eds.), *Geochronology, Time Scales and Global Stratigraphic Correlation*. Spec. Publ.—Soc. Econ. Paleontol. Mineral., 54:129–212.
- Berggren, W.A., and van Couvering, J.A., 1974. The Late Neogene: biostratigraphy, geochronology and paleoclimatology of the last 15 million years in marine and continental sequences. *Palaeogeogr., Palaeoclimatol., Palaeoecol.*, 16:1–216.
- Bukry, D., 1978. Biostratigraphy of Cenozoic marine sediment by calcareous nannofossils. *Micropaleontology*, 24:44–60.
- Bukry, D., 1981. Pacific coast coccolith stratigraphy between Point Conception and Cabo Corrientes, Deep Sea Drilling Project Leg 63. In Yeats, R.S., Haq, B.U., et al., *Init. Repts. DSDP*, 63: Washington (U.S. Govt. Printing Office), 445–471.
- Cita, M.B., 1996a. Report on the 30th International Geological Congress. *Neogene Newsl.*, 3:62–65.
- Cita, M.B., 1996b. Submission of the recommendation for the definition of the Gelasian. *Neogene Newsl.*, 3:49–51.
- Cita, M.B., Rio, D., Hilgen, F., Castradori, D., Lourens, L., and Vergerio, P.P., 1996. Proposal of the global boundary stratotype section and point (GSSP) of the Piacenzian Stage (middle Pliocene). *Neogene Newsl.*, 3:20–47.
- Comas, M.C., Zahn, R., Klaus, A., et al., 1996. *Proc. ODP, Init. Repts.*, 161: College Station, TX (Ocean Drilling Program).
- Crowley, T. J., 1996. Pliocene climates: the nature of the problem. *Mar. Micropaleontol.*, 27:3–12.
- Dowsett, H.J., Barron, J., and Poore, R., 1996. Middle Pliocene sea surface temperatures: a global reconstruction. *Mar. Micropaleontol.*, 27:13–15.
- Fornaciari, E., Di Stefano, A., Rio, D., and Negri, A., 1996. Middle Miocene quantitative calcareous nannofossil biostratigraphy in the Mediterranean region. *Micropaleontology*, 42:37–63.
- Gallagher, L., 1989. Reticulofenestra: a critical review of taxonomy, structure and evolution. In Crux, J.A., and van Heck, S.E. (Eds.), *Nannofossils and Their Applications*: Chichester (Ellis Horwood), 41–75.
- Haq, B.U., Lohmann, G.P., and Wise, S.W., Jr., 1977. Calcareous nannoplankton biogeography and its paleoclimatic implications: Cenozoic of the Falkland Plateau (DSDP Leg 36) and Miocene of the Atlantic Ocean. In Barker, P.F., Dalziel, I.W.D., et al., *Init. Repts. DSDP*, 36: Washington (U.S. Govt. Printing Office), 745–759.
- King, T., 1996. Equatorial Pacific sea surface temperatures, faunal patterns, and carbonate during the Pliocene. *Mar. Micropaleontol.*, 27:63–84.
- Langereis, C.G., and Hilgen, F.J., 1991. The Rosello composite: a Mediterranean and global reference section for the early to early-late Pliocene. *Earth Planet. Sci. Lett.*, 104:211–225.
- Kampfer, E., 1967. Kalkflagellaten-Skelettreste aus Tiefseeschlamm des Sudatlantischen Ozeans. *Ann. Naturhist. Mus. Wien.*, 71:117–198.
- Martini, E., 1971. Standard Tertiary and Quaternary calcareous nannoplankton zonation. In Farinacci, A. (Ed.), *Proc. 2nd Int. Conf. Planktonic Microfossils Roma*: Rome (Ed. Tecnosci.), 2:739–785.
- McIntyre, A., Bé, A.W.H., and Roche, M.B., 1970. Modern Pacific coccolithophorida: a paleontological thermometer. *Trans. N.Y. Acad. Sci.*, 32:720–731.
- Matsuoka, H., and Okada, H., 1989. Quantitative analysis of Quaternary nannoplankton in the subtropical northwestern Pacific Ocean. *Mar. Micropaleontol.*, 14:97–118.

- Müller, C., 1985. Late Miocene to Recent Mediterranean biostratigraphy and paleoenvironments based on calcareous nannoplankton. In Stanley, D.J., and Wezel, F.C. (Eds.), *Geological Evolution of the Mediterranean Basin*: New York (Springer-Verlag), 471–485.
- Pujos, A., 1985. Cenozoic nannofossils, central equatorial Pacific, Deep Sea Drilling Project Leg 85. In Mayer, L., Theyer, F., Thomas, E., et al., *Init. Repts. DSDP*, 85: Washington (U.S. Govt. Printing Office), 581–607.
- Pujos, A., 1987. Late Eocene to Pleistocene medium-sized and small-sized "reticulofenestrads." *Proc. INA Vienna Meeting 1985, Abh. Geol. Bundesanst. (Austria)*, 39:239–277.
- Raffi, I., and Rio, D., 1981. *Coccolithus pelagicus* (Wallich): a paleotemperature indicator in the late Pliocene Mediterranean deep sea record. In Wezel, F.C. (Ed.), *Sedimentary Basins of Mediterranean Margins*: C.N.R. Italian Project of Oceanography, Bologna (TecnoPrint), 187–190.
- Raymo, M.E., Grant, B., Horowitz, M., and Rau, G.H., 1996. Mid-Pliocene warmth: stronger greenhouse and stronger conveyor. *Mar. Micropaleontol.*, 27:313–326.
- Rio, D., and Fornaciari, E., 1994. Remarks on middle to late Miocene chronostratigraphy. *Neogene News.*, 1:26–29.
- Rio, D., Raffi, I., and Villa, G., 1990a. Pliocene–Pleistocene calcareous nannofossil distribution patterns in the Western Mediterranean. In Kastens, K.A., Mascle, J., et al., *Proc. ODP, Sci. Results*, 107: College Station, TX (Ocean Drilling Program): 513–533.
- Rio, D., Sprovieri, R., and Di Stefano, E., 1994. The Gelasian stage: a proposal for a new chronostratigraphic unit of the Pliocene series. *Riv. Ital. Paleontol. Stratigr.*, 100:103–124.
- Rio, D., Sprovieri, R., and Raffi, I., 1984. Calcareous plankton biostratigraphy and biochronology of the Pliocene-lower Pleistocene succession of the Capo Rossello area, Sicily. *Mar. Micropaleontol.*, 9:135–180.
- Rio, D., Sprovieri, R., and Thunell, R., 1991. Pliocene–lower Pleistocene chronostratigraphy: a re-evaluation of Mediterranean type sections. *Geol. Soc. Am. Bull.*, 103:1049–1058.
- Rio, D., Sprovieri, R., Thunell, R., Vergnaud Grazzini, C., and Glaçon, G., 1990b. Pliocene–Pleistocene paleoenvironmental history of the western Mediterranean: a synthesis of ODP Site 653 results. In Kastens, K.A., Mascle, J., et al., *Proc. ODP, Sci. Results*, 107: College Station, TX (Ocean Drilling Program), 695–704.
- Siesser, W. G., 1975. Calcareous nannofossils from the South African continental margin. *GSO/UCT Marine Geol. Prog. Bull.* 5:1–135.
- Siesser, W.G., 1980. Late Miocene origin of the Benguela Upwelling System off northern Namibia. *Science*, 208:283–285.
- Siesser, W.G., 1984. Paleogene sea levels and climates: U.S.A. eastern Gulf Coastal Plain. *Palaeogeogr., Palaeoclimatol., Palaeoecol.*, 47:261–275.
- Siesser, W.G., and Bralower, T.J., 1992. Cenozoic calcareous nannofossil biostratigraphy on the Exmouth Plateau, Eastern Indian Ocean. In von Rad, U., Haq, B.U., et al., *Proc. ODP, Sci. Results*, 122: College Station, TX (Ocean Drilling Program), 601–631.
- Sprovieri, R., 1993. Astrochronology of Pliocene–early Pleistocene Mediterranean calcareous plankton events. *Paleopelagos*, 3:187–194.
- Theodoridis, S., 1984. Calcareous nannofossil biozonation of the Miocene and revision of the helicoliths and discoasters. *Utrecht Micropaleontol. Bull.*, 32:1–271.
- Tribble, J.S., and the Leg 161 Shipboard Scientific Party, 1995. Messinian and early Pliocene sediments of the Western Mediterranean Sea: the transition from an evaporative environment to open marine conditions. *Eos*, 76:7. (Abstract)
- Wei, W., Bergen, J.A., and Applegate, J., 1988. Cenozoic calcareous nannofossils from the Galicia Margin, Ocean Drilling Program Leg 103. In Boillot, G., Winterer, E.L., et al., *Proc. ODP, Sci. Results*, 103: College Station, TX (Ocean Drilling Program), 279–292.
- Young, J.R., 1990. Size variation of Neogene *Reticulofenestra* coccoliths from Indian Ocean DSDP cores. *J. Micropaleontol.*, 9:71–85.
- Young, J.R., 1991. A Quaternary nannofossil range chart. *INA News.*, 13:14–17.

Date of initial receipt: 21 March 1997

Date of acceptance: 19 February 1998

Ms 161SR-241

## APPENDIX

Number of *Coccolithus pelagicus* and *Discoaster brouweri* in Counts of 100 Specimens

Core, section (cm)	<i>C. pelagicus</i>	<i>D. brouweri</i>
Hole 974B		
11H-3, 18-19	100	0
12H-3, 4-5	100	0
12H-CC	92	8
13H-1, 10-11	86	14
13H-3, 27-28	53	47
13H-5, 46-47	88	12
14H-3, 8-9	90	10
14H-CC	96	4
15H-3, 30-31	95	5
15H-CC	96	4
16H-3, 30-31	96	4
16H-CC	100	0
17H-3, 15-16	100	0
17H-CC	100	0
18H-3, 48-49	94	6
18H-CC	92	8
19H-3, 30-31	91	9
19H-CC	87	13
20X-1, 3-4	98	2
20X-3, 57-59	98	2
20X-CC	99	1
21X-3, 10-11	98	2
21X-CC	99	1
22X-3, 17-18	100	0
22X-CC	97	3
Hole 975B		
16H-3, 40-41	100	0
16H-CC	98	2
17X-3, 40-41	96	4
17-CC	100	0
18X-3, 20-21	100	0
18X-CC	92	4
19X-3, 79-80	94	6
19X-CC	92	8
20X-CC	99	1
21X-3, 30-31	94	6
21X-CC	96	4
22X-3, 40-41	98	2
22X-CC	98	2
23X-3, 15-16	92	8
23X-CC	88	12
24X-3, 17-18	94	6
24X-CC	94	6
25X-3, 19-20	94	6
25X-CC	92	8
26X-3, 28-29	93	7
26X-CC	98	2
27X-3, 28-29	100	0
27X-CC	99	1
28X-1, 19-20	96	4
28X-3, 19-20	92	8
28X-CC	97	3
29X-3, 15-16	97	3
29X-5, 15-16	94	6
29X-CC	90	10
30X-3, 30-31	99	1
30X-CC	98	2
31X-3, 47-48	99	1
31X-CC	96	4
32X-3, 70-71	100	0
32X-CC	100	0
33X-CC	94	6
Hole 976B		
49X-CC	100	0
50X-CC	100	0
51X-CC	100	0
52X-CC	100	0
53X-CC	100	0
54X-CC	100	0
55X-CC	100	0
56X-3, 20-21	92	8
56X-CC	95	5
57X-3, 20-21	96	4
57X-CC	97	3
58X-3, 13-14	98	2
58X-CC	98	2
59X-3, 20-21	100	0
59X-CC	97	3

## APPENDIX (continued).

Core, section (cm)	<i>C. pelagicus</i>	<i>D. brouweri</i>	Core, section (cm)	<i>C. pelagicus</i>	<i>D. brouweri</i>
60X-3, 19-20	99	1	15R-CC	100	0
60X-CC	100	0	16R-3, 20-21	98	2
61X-3, 21-22	100	0	16R-CC	97	3
61X-CC	100	0	17R-3, 20-21	100	0
62X-3, 20-21	100	0	17R-CC	100	0
62X-CC	99	1	18R-3, 20-21	99	1
63X-3, 19-20	99	1	18R-CC	97	3
63X-CC	100	0	19R-3, 19-21	98	2
64X-3, 20-21	100	0	19R-5, 19-21	94	6
64X-CC	99	1	19R-CC	84	16
65X-3, 20-21	100	0	20R-1, 20-21	86	14
65X-CC	100	0	20R-3, 20-21	94	6
66X-3, 20-21	99	1	20R-5, 20-21	92	8
66X-CC	100	0	21R-CC	77	23
67X-3, 20-21	99	1	21R-1, 20-21	80	20
67X-CC	100	0	21R-3, 20-21	90	10
68X-CC	99	1	21R-CC	96	4
69X-2, 18-19	100	0	22R-3, 17-18	93	7
69X-CC	99	1	22R-CC	95	5
70X-3, 21-22	99	1	23R-3, 20-21	99	1
70X-CC	99	1	23R-CC	98	2
71X-3, 21-22	98	2	24R-3, 23-24	100	0
71X-CC	100	0	24R-CC	97	3
72X-CC	100	0	25R-3, 20-21	100	0
73X-CC	100	0	25R-CC	99	1
74X-CC	100	0	26R-3, 20-21	100	0
75X-CC	100	0	26R-CC	98	2
Hole 977A			27R-1, 20-21	98	2
34X-CC	100	0	27R-3, 20-21	85	15
35X-CC	100	0	27R-5, 22-23	100	0
36X-CC	100	0	27R-CC	98	2
37X-CC	100	0	28R-3, 20-21	96	4
38X-CC	100	0	28R-CC	89	11
39X-CC	100	0	29R-3, 19-20	96	4
40X-3, 20-21	100	0	29R-CC	100	0
40X-CC	99	1	30R-3, 20-21	94	6
41X-3, 23-24	95	5	30R-CC	99	1
41X-CC	94	6	31R-3, 20-21	100	0
42X-3, 20-21	99	1	31R-CC	100	0
42X-CC	93	7	32R-3, 19-20	99	1
43X-3, 20-21	97	3	32R-CC	100	0
43X-CC, 20-21	98	2	33R-3, 20-21	100	0
44X-1, 19-20	96	4	33R-CC	100	0
44X-3, 20-21	84	16	34R-3, 20-21	100	0
44X-CC	90	10	34R-CC	100	0
45X-3, 20-21	95	5	Hole 979A		
45X-CC	91	9	45X-CC	100	0
46X-3, 20-21	97	3	46X-CC	100	0
46X-5, 20-21	98	2	47X-CC	100	0
46X-CC	96	4	48X-CC	100	0
47X-3, 20-21	100	0	49X-3, 20-21	100	0
47X-CC	100	0	49X-CC	100	0
48X-3, 17-18	100	0	50X-3, 20-21	100	0
48X-CC	96	4	51X-3, 21-23	100	0
49X-3, 20-21	100	0	51X-CC	100	0
49X-CC	97	3	52X-3, 15-16	100	0
50X-3, 18-19	94	6	52X-CC	100	0
50X-5, 22-23	100	0	53X-1, 23-24	98	2
50X-CC	100	0	53X-3, 23-24	81	19
51X-3, 18-19	100	0	53X-5, 20-21	88	12
51X-CC	98	2	53X-CC	99	1
52X-3, 22-23	100	0	54X-3, 22-24	99	1
52X-CC	100	0	54X-5, 23-24	90	10
53X-3, 20-21	100	0	54X-CC	77	23
53X-CC	96	4	55X-1, 21-22	86	14
54X-3, 22-23	96	4	55X-3, 22-23	94	6
54X-CC	95	5	55X-CC	98	2
55X-3, 21-22	100	0	56X-3, 20-21	98	2
55X-5, 21-22	96	4	56X-CC	99	1
55X-CC	94	6	57X-3, 21-22	99	1
56X-3, 20-21	100	0	57X-CC	97	3
56X-CC	100	0	58X-3, 19-20	94	6
57X-1, 21-22	98	2	58X-CC	98	2
Hole 978A			59X-3, 20-21	99	1
11R-3, 20-21	100	0	59X-CC	99	1
11R-5, 20-21	98	2	60X-3, 19-20	96	4
11R-CC	98	2	60X-CC	96	4
12R-3, 20-21	100	0	61X-1, 22-23	94	6
12R-CC	99	1	61X-3, 19-20	84	16
13R-3, 20-21	100	0	61X-5, 19-20	86	14
13R-CC	100	0	61X-CC	95	5
14R-3, 20-21	100	0	62X-3, 21-22	93	7
14R-CC	100	0	62X-CC	91	9
15R-3, 20-21	99	1			